IMPROVEMENT OF THE DISMC METHOD VIA ISMC TO PROVIDE A FASTER RESPONSE TIME AND MITIGATE CHATTERING PHENOMENON

Lachtar SALAH[1], Bourbia WAFA[2], Neçaibia AMMAR[3], Bouraiou AHMED[4], Ziane ABDERREZZAQ[5]

The presence of a Maximum Power Point Tracking (MPPT) algorithm in a PV system is driving the process at a Maximum Power Point (MPP) is mandatory since the PV array feature is non-linear and variable with changing climatic conditions, as a result, the maximum power generated is obtained. In this paper, a new robust MPPT technique proposes using the notion of a double integral sliding mode controller (DISMC) for a standalone PV system. The goal of this super-slide algorithm is to design a new sliding surface that will help improve slow transient response and mitigate chattering phenomenon compared to integral ISMC. The study permits compare both algorithms to get the best algorithm in terms of time response and the chattering phenomenon, in addition to efficiency, stability, and robustness. The modeling of the stand-alone PV system and the simulations were carried out using Matlab/Simulink.

Keywords: Standalone PV system, MPPT, DC-DC boost converter, ISMC, DISMC

1. Introduction

Up to now, fossil fuels (petroleum, coal, natural gas, nuclear, etc.) remain the main sources of energy production to cover the annual growing global demand, which has negative repercussions on the environment. These negative impacts resulting from greenhouse gas emissions contributed to climate change, which caused many natural disasters and became the most serious problem that

[1] Ph.D., Unité de Recherche en Energie Renouvelables en Milieu Saharien, URERMS, Centre de Développement des Energies Renouvelables, CDER, Adrar, Algeria, e-mail: lachtarsalahba@gmail.com
[2] Ph.D., Dept. of Science and technology, University of Adrar, National Road N°6 Adrar 01000, Algeria, e-mail: bourbiawafabm@gmail.com
[3] Ph.D., Unité de Recherche en Energie Renouvelables en Milieu Saharien, URERMS, Centre de Développement des Energies Renouvelables, CDER, Adrar, Algeria, e-mail: necaibia.ammar@gmail.com
[4] Ph.D., Unité de Recherche en Energie Renouvelables en Milieu Saharien, URERMS, Centre de Développement des Energies Renouvelables, CDER, Adrar, Algeria, e-mail: bouraiouahmed@gmail.com
[5] Ph.D., Unité de Recherche en Energie Renouvelables en Milieu Saharien, URERMS, Centre de Développement des Energies Renouvelables, CDER, Adrar, Algeria, e-mail: abderrezzaq.ziane@gmail.com

directs humanity in this century, which threatens life on our planet. To reduce pollution, limit the consequences of climate change, and given the present development in the standard of living in the world. The huge increase in energy demand has pushed many countries of the world to tend to develop renewable energies, especially photovoltaic, wind, thermal, hydraulic energy, as a result of the giant leap in the field of industry and modern technology, considering that energy is the lifeblood of all world economies. Besides, it has become a feature of this era and an alternative to fossil fuels that are crumbling, which embodies the clauses of the Kyoto Protocol and later, Paris Climate Agreement [1], [2].

Recently, solar energy has become a reliable source of energy with the continuous decline in the production rate and the cost of maintenance thanks to the technological progress and the development of the PV market. In this regard, the World Solar Growth (WSG) expects a growth rate of 7% in the period from 2020 to 2025, which is approximately 8 GW/year, with a total solar capacity of 687 GW that will be added during this period [3].

The development and digitization of power electronics technology in the field of photovoltaics has allowed the rapid development of photovoltaic applications, as it is considered an ideal solution as a renewable energy source that can be used in isolated rural and desert areas that are generally far from the public electricity grid or integrated into grid-connected applications.

The Maximum Power Point Tracking (MPPT) control study of the DC/DC phase under variable weather conditions with time is based on the level of radiation and temperature. In this regard, many algorithms have been proposed for the optimal tracking of MPP. The most popular and most used application in MPP is the Perturb and Observe (P&O) algorithm, due to its implementation simple and easy [4]–[6]. But the P&O algorithm weakness is evident when large fluctuations appear around the MPP in a steady-state, which in turn affects the power signals that appear on them with undesired ripples and which represent an obstacle when operating the PV system, as P&O has difficulty tracking properly during sudden radiation changes. Therefore, P&O technology is sensitive to radiation changes and lacks robustness. For this purpose, in the last decade, many researchers all over the world have developed many MPPT algorithms able to track MPP even upon the sudden change in radiation. To eliminate or mitigate these shortcomings, the focus is mainly on the performance of these controllers to improve overshoot and time convergence, and on robustness in face of climatic changes. Among the papers cited in literature. Sher et al relied on a comparison of the instantaneous and incremental conductance values of the photovoltaic generator, where the optimum value is reached when the two values are equal. This IC technique performs well under rapidly variated climatic conditions and fluctuations around MPP are almost insignificant. However, under partially shad conditions, it is unable to track MPP [7]. Fractional Open Circuit Voltage algorithm and

Fractional Short Circuit Current respectively presented in [8], those techniques are simplified. The first is centered on the linear relationship between Voc and the output maximum Vmpp, and the second is centered on a relationship between the current Isc and the current at maximum power point Impp.

Also, many intelligent MPPT technologies have been proposed for MPP tracking with fast response and insignificant oscillations. Mentioning among them, Ziane et al. proposed the FL-based MPPT algorithm. This algorithm has been compared to an IC-based MPPT algorithm in terms of speed and precision [9]. Loubna et al. presented an ANN-based MPPT algorithm for PV systems under partially shad conditions. This method compared with P&O and IC controller based on a fuzzy duty cycle change estimator to prove the effectiveness in tracking MPP and providing a faster response time [10].

Sliding mode control (SMC) appeared in the Soviet Union in the last century by Utkin (1977) [11], it's considered as a nonlinear control method belonging to the family of the variable structure systems theory. This technique has successfully applied in DC-DC converters thanks to its simplicity of implementation, robustness against parameter variations, and good dynamic response. Many MPPT algorithms based on conventional sliding mode have been proposed [12]–[14]. The stabilization control, quantized along a bounded margin of parametric imprecision, brings the operating point close to the sliding surface, which is an image of the MPP optimum area. The implementation of the sliding mode is a simple and low cost, but the phenomenon of chattering and slow transient response remain major drawbacks, leading researchers to suggest other higher-order sliding mode MPPT algorithms to overcome the aforementioned drawbacks [11], [15], [16].

The main objective of this paper is to eliminate the phenomenon of chattering and slow time response. To patch up this gap, a double integral sliding mode-based MPPT algorithm was used. A simulation comparison study between conventional Sliding Mode Control including an integral component to Smoothing the chattering phenomenon (SSMC) which was proposed by Salah et al. (2019) [17], and double integral sliding mode-based MPPT algorithm for the standalone PV system. Modeling and simulation in a Matlab/Simulink environment are used for both techniques to prove which is the best in terms of response time and without chattering phenomenon in light of the natural weather changes which are sudden and rapid.

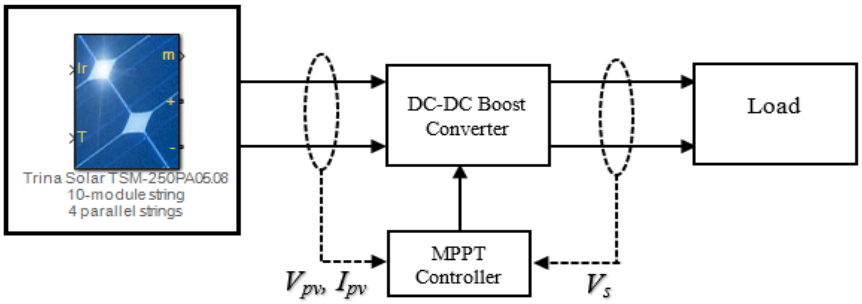

Fig. 1. DC-DC Boost converter connecting PV system with DISMC-based MPPT controller

2. Photovoltaic array modeling and characteristics

Photovoltaics is one of the best ways to generate electrical energy by using solar cells to convert solar energy into a flow of electrons. The effect of photovoltaics is due to light photons stimulating electrons to move from a lower energy level to a higher energy level and thus obtain electric power.

To understand the behavior of the solar cell, it is necessary to create an equivalent electrical model presented in Fig. 1, which is based on known electrical components that are easy to study and analyze. An ideal solar cell may be designed with a current generator source Iph in parallel with a diode D. But practically no solar cell is perfect, so a parallel resistance Rsh and a serial resistance Rs as a simulation model for the cell.

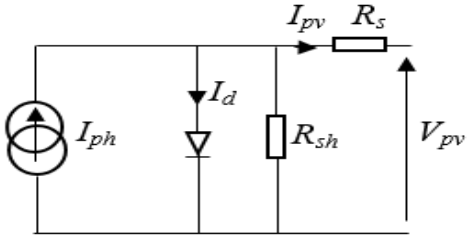

Fig. 2. PV cell equivalent circuit

From the equivalent circuit, it is clear that the current produced by the solar cell is equal to the current produced by the source current, counting the current that flows through the diode, and the current that flows through the parallel resistance having neglected value.

The equations of the equivalent one diode model for the nonlinear I-V characteristic of the PV cell shown in Fig .2 are presented as follows [18], [19]:

$$I_{pv} = I_{ph} - I_d - I_{sh} = I_{ph} - I_0 \left\{ \exp\left[\left(V_{pv} + I_{pv} R_s \right) / aV_T \right] - 1 \right\} - \left(V_{pv} + I_{pv} R_s \right) / R_{sh} \quad (1)$$

Diode current equation is:

$$I_d = I_0 \left\{ \exp\left[V_j / aV_T \right] - 1 \right\}, \; V_j = V_{pv} + I_{pv} R_s \; , \; V_T = KT / q \quad (2)$$

$$I_0 = I_{rs}\left[T / T_r\right]^3 \exp\left[\left(\left(qE_{g_0} / aK\right) - \left(1/T_r - 1/T\right)\right)\right] \quad (3)$$

Shunt current equation is:

$$I_{sh} = \left(V_T / R_{sh}\right) = \left(\left(V_{pv} + I_{pv}R_s\right) / R_{sh}\right) \quad (4)$$

Where:

I_{pv} : output current of the PV cell (A).

I_{ph} : photogenerated current (A).

I_0 : reverse saturation current (A).

I_{rs} : saturation current at reference temperature (A).

V_{pv} : output voltage of the PV cell (V).

V_j : voltage across both diode and resistance R_{sh} (V).

V_T : the thermal voltage. At 25 °C, $V_T \approx 0.0259 volt$.

a : diode ideality factor (1 for an ideal diode).

I_d : diode current (A).

I_{sh} : shunt current (A).

R_s : series resistance of cell $\left(\Omega\right)$.

R_{sh} : parallel resistance of cell $\left(\Omega\right)$.

q : electron charge.

K : Boltzmann's constant.

T : absolute temperature (K).

T_r : reference temperature (K).

The main specifications of the PV module are shown in Table 1.

Table 1

PV ARRAY SPECIFICATION

Parameters	Value
PV module per string	10
Parallel connected strings	4
Cells per module (Ncell)	60
Open circuit voltage Voc (V)	37.6
Short circuit current Isc (A)	8.55
Voltage at MPP Vmp (V)	31
Current at MPP Imp(A)	8.06
Maximum power per module (w)	249.86

3. Solar irradiation and temperature effect on the PV module behavior

PV module behavior is usually very sensitive to solar irradiance variations and temperature because these variations have a significant effect on the power supplied by the module. Fig. 3 shows that for a constant temperature of 25° C, I_{pv} and P_{pv} as a function of V_{pv} for different irradiance values give many curves P(V) corresponding to the maximum power point (V_{mp}, I_{mp}). So, I_{sc} varies proportionally to the solar irradiance. Whereas, V_{oc} varies very slightly [20].

Fig. 4 shows that for a constant irradiance of 1000 W/m^2, and the temperature varies ascendency, V_{oc} decreases and I_{sc} varies slightly. Therefore, PV module operation mainly depends on the weather conditions to which it is exposed. For this purpose, it must be taken into consideration these factors in

order to correctly determine the PV generator size, allowing the required power to be obtained [20].

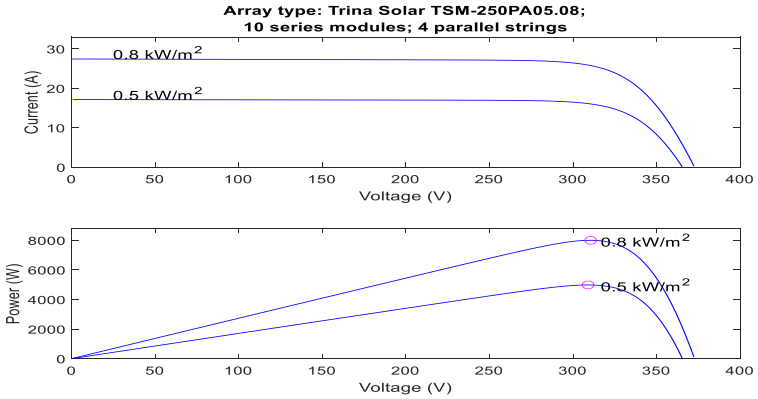

Fig. 3. I-V and P-V characteristics at 25°C and specified solar irradiances

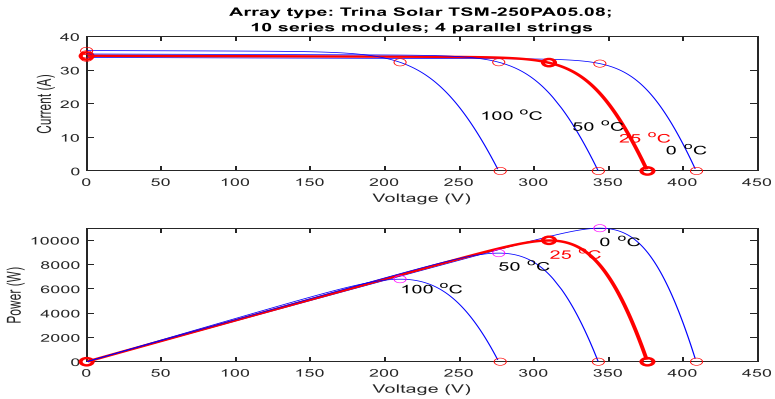

Fig. 4. I-V and P-V characteristics at 1000 W/m^2 and specified temperatures

4. DC-DC boost converter modeling

Fig. 5 shows a boost converter that raises the DC input voltage to a higher output voltage. This boost converter includes a switch (*S*), an inductance (L), a diode shielding *S* as it prevents return current, and the capacitor C_2 filtering the output voltage.

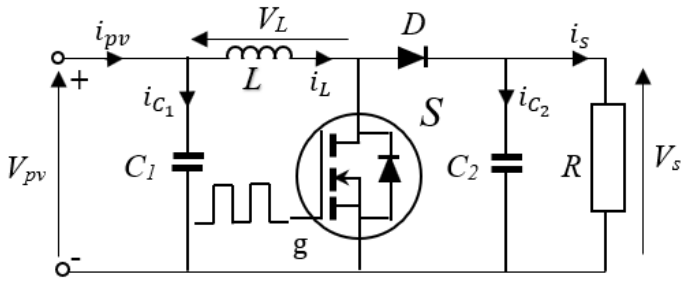

Fig. 5. DC-DC boost converter

According to Fig. 5, when the switch *S* is ON, the diode is reversely polarized. The inductance L loads and the current carried by the source start to increase gradually. In this first case, a set of equations is illustrated as follows:

$$\begin{cases} \dot{V}_L = i_{C_1} / C_1 = \left(i_{pv} - i_L\right) / C_1 \\ \dot{V}_s = i_{C_2} / C_2 = -i_s / C_2 \\ \dot{I}_L = V_L / L = V_{pv} / L \end{cases} \tag{5}$$

When *S* is OFF and L releases the stored voltage, which is added to the source voltage to supply the load. In this second case, a set of equations is illustrated as follows:

$$\begin{cases} \dot{V}_{pv} = i_{C_1} / C_1 = \left(i_{pv} - i_L\right) / C_1 \\ \dot{V}_s = i_{C_2} / C_2 = -\left(i_L - i_s\right) / C_2 \\ \dot{I}_L = V_L / L = \left(V_{pv} - V_s\right) / L \end{cases} \tag{6}$$

With both sets of equations (5) and (6) mentioned above, it is easy to establish the following equation:

$$V_{pv}.D = \left(V_s - V_{pv}\right).\left(1 - D\right) \tag{7}$$

The conversion report is written as follows:

$$V_s / V_{pv} = 1/\left(1 - D\right) \quad D \in \left[0 \quad 1\right] \tag{8}$$

5. Double integral sliding mode-based MPPT control

For maximum output power, the proposed DISMC-based MPPT model is implemented in Matlab/Simulink. This algorithm was developed in order to eliminate the chatter, which is a nuisance, where unwanted disturbances occur in PV systems. The sliding mode control system consists of two main parts, the first part is to extract the sliding surface through the parameters provided by DC-DC, the second part is the formulation of the control law to drive and maintain the system towards sliding surface.

The sliding mode $S(t)$ is defined by:

$$S(t) = \left\{ x \setminus S(x,t) = \dot{S}(x,t) = 0 \right\} \tag{9}$$

The sliding surface is selected in such a way as to provide the maximum power output. The sliding surface is defined by:

$$\left(\partial P_{pv} / \partial I_{pv}\right) = 0, \quad \left(\partial P_{pv} / \partial I_{pv}\right) = I_{pv}\left(\left(\partial V_{pv} / \partial I_{pv}\right) + \left(V_{pv} / I_{pv}\right)\right) \tag{10}$$

The sliding surface is as follow:

$$S(t,x) = \left(\left(\partial V_{pv} / \partial I_{pv}\right) + \left(V_{pv} / I_{pv}\right)\right) \tag{11}$$

For the design of the controller, the tracking error e is given as follow:

$$S(x)=e(x),\ e(x)=e(x_1)+e(x_2) \tag{12}$$

$$e(x_1)=\int\left(\Delta P/\Delta I\right)dt,\ e(x_2)=\int\left\{\int\left(\Delta P/\Delta I\right)dt\right\}dt,\ \begin{cases}\Delta P=P_{pv}(k)-P_{pv}(k-1)\\ \Delta I=I_{pv}(k)-I_{pv}(k-1)\end{cases} \tag{13}$$

Generally, the sliding mode control law is made up of two terms, the equivalent control term u_{eq} and the discontinuous control term u_n. The DISMC algorithm is used to stabilize the system and push it to achieve convergence to the desired path at the right time.

$$u=u_{eq}+u_n \tag{14}$$

In order to obtain equivalent control u_{eq}, the condition of stability must be provided.

$$\begin{cases}S(x)=0\\ \dot{S}(x)=0\end{cases}\Rightarrow u\cong u_{eq} \tag{15}$$

The equivalent control u_{eq} can be obtained by solving the following algebraic equation:

$$\dot{S}=\left[dS/dx\right]^T,\quad \dot{x}=\left[dS/dx\right]^T.\left(f(x)+g(x)u_{eq}\right)=0 \tag{16}$$

$$u_{eq}=-\left(\left[dS/dx\right]^T\ f(x)\right)/\left(\left[dS/dx\right]^T\ g(x)\right)=1-\left(K_1\int S+V_{pv}\right)/V_s \tag{17}$$

Taking into account that the discontinuous control u_n to ensure the Lyapunov's stability criterion is possible, which is given given by:

$$S(x).\dot{S}(x)<0 \tag{18}$$

The expression of the discontinuous control law u_n is given by:

$$u_n=K_2.\left|S\right|^{\alpha}.\sin g(S),\quad 0<\alpha<1 \tag{19}$$

$$\begin{cases}\sin g(S)=1 \quad if\ S(x)>0\\ \sin g(S)=0 \quad if\ S(x)=0\\ \sin g(S)=-1\ if\ S(x)<0\end{cases} \tag{20}$$

$$u=u_{eq}+u_n=\left[1+K_2.\left|S(x)\right|^{\alpha}.\sin g(S)-\left(K_1\int S(x)dx+V_{pv}\right)/V_s\right] \tag{21}$$

Where K_1 and K_2 are positive constants

6. Simulation results and discussion

To carry out this study, we have selected four parallel strings and ten series-connected modules per string using a Trina Solar STM-250PA05.08 PV module have been selected as a PV power source.

In addition to the PV system specifications given in Table 1, the boost converter parameters for the simulation are L = 0.5 mH, C1 = 220 uF, C2 = 330 uF, and R = 26 Ω. The proposed MPPT method is appraised from some above-mentioned factors such as transient response, chattering phenomena, and robustness to weather changes. Different values of solar irradiance and temperature are taken in both the DISMC and ISMC methods, and the results are compared in order to show the robustness and fast transient response.

6.1 In temperature change case

The PV system operates in the ideal condition where the temperature level is 25 °c in the first and the end interval [0, 1] sec & [2, 4] sec, then the temperature changes in the extended time from [1, 2] sec, where the temperature level is 30 °c as shown in Fig. 6.

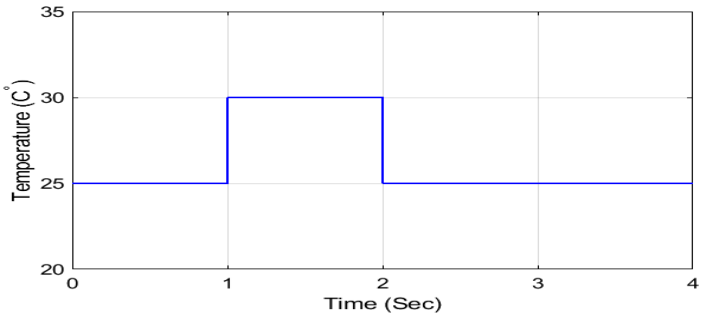

Fig. 6. Temperature change

The PV system shows fast response, low chattering, and good tracking performance in the case of the DISMC algorithm compared to the ISMC algorithm as shown in the zoom, as appears the data statistics for Ppv Fig.7 (a) in the first row at t=0 sec Ppv=2.944Wt for DISMC, while for ISMC the power Ppv= 0.9814Wt at t=0, Which clearly shows the response is three time faster in the transient mode (0.9814*3=2.9442Wt), the Ppv(DISMC) maximum value at t = 4 sec Ppv= 9999 Wt a difference of 3 Wt compared to the Ppv(ISMC) i.e. good tracking performance, and the standard deviation (std) in the sixth row at t = 1.155 sec Ppv-std=307.8Wt for the DISMC which proved that the chattering phenomenon is weak compared to the ISMC which Ppv-std=620.3Wt. Almost the same for the Vpv (Fig.7 (b)) and Ipv (Fig.7 (c)) data statistics, where the DISMC always gives results better than the ISMC in terms of response, chattering phenomenon, and tracking performance.

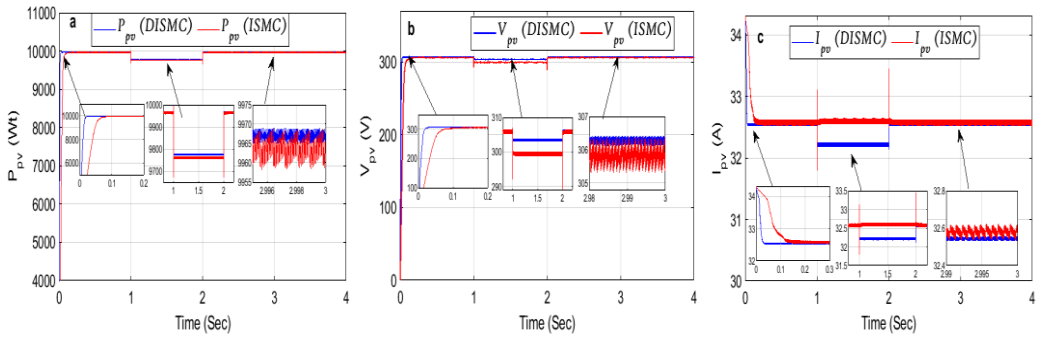

Fig. 7. Temperature variation: a) P_{pv} power, b) V_{pv} voltage, c) I_{pv} current,

6.2 In solar irradiance change case

Regarding the evaluation of both methods, and a comparison between them, in order to demonstrate the robustness in the case of changing the solar irradiance, the value of the solar irradiance 1000 W/m^2 is taken at the beginning and the end of time interval [0, 1] sec & [2, 4] sec, while a lower value of 800 W/m^2 is taken for time interval [1, 2] sec (Fig. 8).

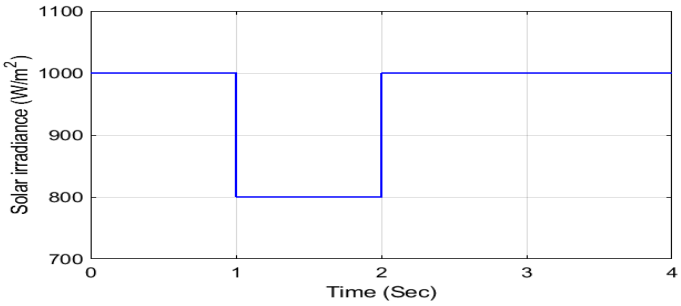

Fig. 8. Solar irradiance change

Figs. 9 show the tracking results for Ppv, Vpv, and Ipv respectively in the case of solar irradiance change while keeping the temperature constant at the ideal value of 25°C. The system reaches the steady-state mode very quickly, that is in a very short time, almost neglected in the different levels of irradiance for both MPP methods. However, the DISMC method remains has the fastest transient response in the case of the beginning (at t = 0 sec) and does not appear shattering phenomenon at t = 1 sec compared to the ISMC method which is clearly shows shattering phenomenon (Fig.9 (a)). In addition, large fluctuations in the steady-state as shown in the zoom.

According to the statistics data given in Fig.9 (a), DISMC is 3 times faster at start-up time (t = 0 s) as it equals 2.944 Wt compared to ISMC which is equivalent to 2.944 / 3 = 0.981 Wt. The maximum Ppv power reaches the nominal Ppv power of the system which is equal to 9999 Wt in steady state at t = 4 sec for the DISMC method. While in the case of ISMC method, Ppv does not exceed

9976 Wt, which is the maximum power at the same time mentioned above. On the other hand, the MPP for voltage and current are the same for both methods according to the statistics data shown in Fig.9 (b) and (c) respectively. Faster at start-up time, low oscillations, and no chattering phenomenon in both quantities (Vpv and Ipv) for DISMC compared to the ISMC.

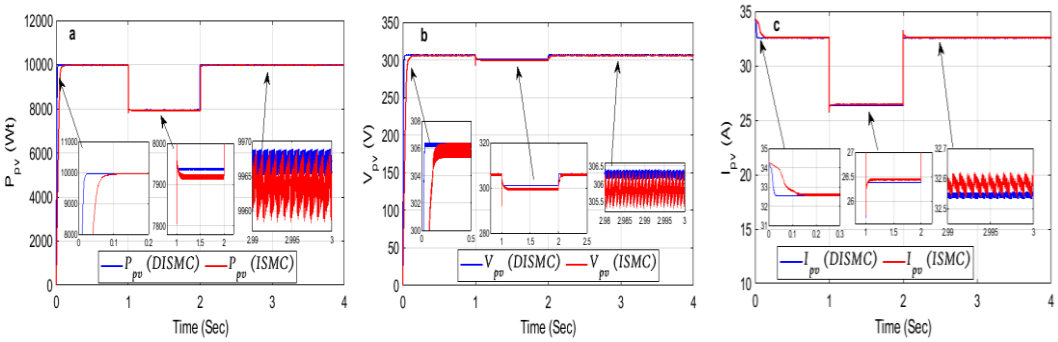

Fig. 9. Irradiance variation: a) P_{pv} power, b) V_{pv} voltage, c) I_{pv} current,

7. Conclusion

This paper presents the comparison between both DISMC and ISMC technics applying on a standalone PV system to appear the best performances knowing fast convergence, a fast transient response, and robustness to climate condition variation such as the irradiance or the temperature. Both technics are verified via simulations under Matlab/Simulink environment. The Lyapunov approach was used to ensure the stability of the controlled system. The comparison provided a clear reading that the DISMC based MPPT is better than the ISMC based MPPT in terms of performance, a fast transient response, a weak chattering phenomenon, and robustness to climate condition variation, which is clearly showed in the data statistics. The rapid advancement of technology will provide the future of such works as it will enable the development of more effective methods of obtaining an ideal MPPT.

R E F E R E N C E S

[1] B. Ki-moon, “Kyoto Protocol Reference Manual,” United Nations Framew. Conv. Clim. Chang., p. 130, 2008, doi: 10.5213/jkcs.1998.2.2.62.

[2] J. Delbeke, A. Runge-Metzger, Y. Slingenberg, and J. Werksman, “The paris agreement,” Towar. a Clim. Eur. Curbing Trend, pp. 24–45, 2019, doi: 10.4324/9789276082569-2.

[3] Https://www.spglobal.com/platts/en/market-insights/latest-news/electric-power/111720-global-solar-growth-seen-7-higher-for-2020-2025-period-platts-analytics, “09/03/2021.”

[4] S. Salman, X. Ai, and Z. Wu, “Design of a P-&-O algorithm based MPPT charge controller for a stand-alone 200W PV system,” Prot. Control Mod. Power Syst., vol. 3, no. 1, 2018, doi: 10.1186/s41601-018-0099-8.

[5] C. T. Phan-Tan and N. Nguyen-Quang, “A P&O MPPT method for photovoltaic applications based on binary-searching,” IEEE Int. Conf. Sustain. Energy Technol. ICSET, vol. 0, pp. 78–82, 2017, doi: 10.1109/ICSET.2016.7811760.

[6] M. L. Azad, S. Das, P. Kumar Sadhu, B. Satpati, A. Gupta, and P. Arvind, "P&O algorithm based MPPT technique for solar PV system under different weather conditions," Proc. IEEE Int. Conf. Circuit, Power Comput. Technol. ICCPCT 2017, pp. 0–4, 2017, doi: 10.1109/ICCPCT.2017.8074225.

[7] H. A. Sher, A. F. Murtaza, A. Noman, K. E. Addoweesh, K. Al-Haddad, and M. Chiaberge, "A New Sensorless Hybrid MPPT Algorithm Based on Fractional Short-Circuit Current Measurement and P&O MPPT," IEEE Trans. Sustain. Energy, vol. 6, no. 4, pp. 1426–1434, 2015, doi: 10.1109/TSTE.2015.2438781.

[8] N. A. Kamarzaman and C. W. Tan, "A comprehensive review of maximum power point tracking algorithms for photovoltaic systems," Renew. Sustain. Energy Rev., vol. 37, pp. 585–598, 2014, doi: 10.1016/j.rser.2014.05.045.

[9] A. Ziane, A. Necaibia, M. Mostfaoui, A. Bouraiou, N. Sahouane, and R. Dabou., "A Fuzzy Logic MPPT For Three-Phase Grid-Connected PV Inverter," in Twentieth International Middle East Power Systems Conference (MEPCON), 2018, pp. 383–388, doi: 10.1109/MEPCON.2018.8635211.

[10] L. Bouselham, M. Hajji, B. Hajji, and H. Bouali, "A New MPPT-based ANN for Photovoltaic System under Partial Shading Conditions," Energy Procedia, vol. 111, no. September 2016, pp. 924–933, 2017, doi: 10.1016/j.egypro.2017.03.255.

[11] A. Kchaou, A. Naamane, Y. Koubaa, and N. M'sirdi, "Second order sliding mode-based MPPT control for photovoltaic applications," Sol. Energy, vol. 155, pp. 758–769, 2017, doi: 10.1016/j.solener.2017.07.007.

[12] H. Yatimi and E. Aroudam, "Assessment and control of a photovoltaic energy storage system based on the robust sliding mode MPPT controller," Sol. Energy, vol. 139, pp. 557–568, 2016, doi: 10.1016/j.solener.2016.10.038.

[13] C. S. Chiu, Y. L. Ouyang, and C. Y. Ku, "Terminal sliding mode control for maximum power point tracking of photovoltaic power generation systems," Sol. Energy, vol. 86, no. 10, pp. 2986–2995, 2012, doi: 10.1016/j.solener.2012.07.008.

[14] K. M. Nacer, N. Bechara, and M. Abarkan, "The VSAS approach gives the Best MPPT for Solar Energy Sources," Renew. Energy Sustain. Dev., vol. 1, no. 1, pp. 60–71, 2015.

[15] R. Pradhan and B. Subudhi, "Double Integral Sliding Mode MPPT Control of a Photovoltaic System," IEEE Trans. Control Syst. Technol., vol. 24, no. 1, pp. 285–292, 2016, doi: 10.1109/TCST.2015.2420674.

[16] S. C. Tan, Y. M. Lai, and C. K. Tse, "Indirect sliding mode control of power converters via double integral sliding surface," IEEE Trans. Power Electron., vol. 23, no. 2, pp. 600–611, 2008, doi: 10.1109/TPEL.2007.915624.

[17] S. Lachtar, A. Bouraiou, O. D. And, and R. Maouedj, "Smooth Sliding Mode-Based MPPT Algorithm for Photovoltaic Applications," in 1st Global Power, Energy and Communication Conference (GPECOM), Nevsehir, Turkey, 2019, p. 253–258, doi: 10.1109/GPECOM.2019.8778484.

[18] N. Yildiran and E. Tacer, "Identification of photovoltaic cell single diode discrete model parameters based on datasheet valuesYildiran, N., & Tacer, E. (2016). Identification of photovoltaic cell single diode discrete model parameters based on datasheet values. Solar Energy, 127, ," Sol. Energy, vol. 127, pp. 175–183, 2016.

[19] H. H. Ammar, A. T. Azar, R. Shalaby, and M. I. Mahmoud, "Metaheuristic Optimization of Fractional Order Incremental Conductance (FO-INC) Maximum Power Point Tracking (MPPT)," vol. 2019, 2019.

[20] M. Chegaar, A. Hamzaoui, A. Namoda, P. Petit, M. Aillerie, and A. Herguth, "Effect of illumination intensity on solar cells parameters," Energy Procedia, vol. 36, pp. 722–729, 2013, doi: 10.1016/j.egypro.2013.07.084.